LED-based multi-wavelength phase imaging interference microscopy

N. Warnasooriya and M. K. Kim

Department of Physics, University of South Florida, Tampa, FL 33620
nwarnaso@mail.usf.edu

Abstract: LED-based multi-wavelength phase imaging interference microscopy combines phase-shifting interferometry with multi-wavelength optical phase unwrapping. This technique consists of a Michelson-type interferometer illuminated with a LED. The reference mirror is dithered for obtaining interference images at four phase quadratures, which are then combined to calculate the phase of the object surface. The 2π ambiguities are removed by repeating the experiment using two or more LEDs at different wavelengths, which yields phase images of effective wavelength much longer than the original. The resulting image is a profile of the object surface with a height resolution of several nanometers and range of several microns. The interferographic images using broadband sources are significantly less affected by coherent noise.

© 2007 Optical Society of America

OCIS codes: (120.3180) Interferometry; (120.5050) Phase measurement; (180.3170) Interference microscopy

References and links

1. E. D. Barone-Nugent, A. Barty, K. A. Nugent, "Quantitative phase amplitude microscopy I: optical microscopy," J. Microscopy **3**, 194-203 (2002).
2. C. J. Mann, L. Yu, C. Lo and M. K. Kim, "High-resolution quantitative phase-contrast microscopy by digital holography," Opt. Express **13**, 8693-8698 (2005).
3. P. Marquet, B. Rappaz, T. Colomb, F. Charriere, J. Kuhn, Y. Emery, E. Cuche, C. Depeursinge, P. Magistretti, " Digital holographic microscopy, a new optical imaging technique to investigate cellular dynamics," in *Biophotonics and New Therapy* Frontiers, R. Grzymala and O. Haeberle, eds.,Proc. SPIE **6191**, 61910U-61910U5 (2006).
4. Y. Park, G. Popescu, K. Badizadegan, R. R. Dasari and M. S. Feld, "Diffraction phase and fluorescence microscopy," Opt. Express **14**, 8263-8268 (2006).
5. M. Servin, J.L. Marroquin, D. Malacara and F.J. Cuevas, "Phase unwrapping with a regularized phase-tracking system," Appl. Opt. **37**, 1917-1923 (1998).
6. Yeou-Yen Cheng and James C. Wyant, "Multiple-wavelength phase-shifting interferometry," Appl. Opt. **24**, 804-807 (1985).
7. C. Wagner, W. Osten and S. Seebacher, "Direct shape measurement by digital wavefront reconstruction and multiwavelength contouring," Opt. Eng. **39**, 79-85, (2000).
8. J. Gass, A. Dakoff, M.K. Kim, "Phase imaging without 2π ambiguity by multiwavelength digital holography," Opt. Lett., **28**, 1141-1143, (2003).
9. D. Parshall and M. K. Kim, "Digital holographic microscopy with dual wavelength phase unwrapping," App. Opt., **45**, 451-459 (2006).
10. M. Tziraki, R. Jones, P. M. W. French, M. R. Melloch and D. D. Nolte, "Photorefractive holography for imaging through turbid media using low coherent light," Appl. Phy. B, **70**, 151-154 (2000).
11. S. Dilhaire, S. Grauby, S. Jorez, L. D. P. Lopez, J. Rampnoux and W. Claeys, " Surface displacement imaging by interferometry with a light emitting diode," Appl. Opt. **41**, 4996-5001 (2002).
12. L. Repetto, E. Piano and C. Pontiggia, "Lensless digital holographic microscope with light-emitting diode illumination," Opt. Lett. **29**, 1132-1134 (2004).
13. A. Fercher, W. Drexler, C. K. Hitzenberger and T. Lasser, "Optical coherence tomography-principles and applications," Rep. Prog. Phys. **66**, 239-303 (2003).
14. Luxeon™ Emitter and Star sample information AB11, 2 (Feb 2002).

#83569 - $15.00 USD Received 30 May 2007; revised 10 Jul 2007; accepted 10 Jul 2007; published 12 Jul 2007
(C) 2007 OSA

1. Introduction

Most biological specimens are hardly absorptive, lacking sufficient contrast for standard bright-field microscopy. Several widely used phase imaging techniques are Zernike phase contrast (ZPC) microscopy, differential interference contrast (DIC) microscopy and Hoffman modulation contrast (HMC) microscopy. The Zernike phase contrast technique converts changes in phase into corresponding changes in amplitude by using a phase plate. ZPC uses common path interferometry, where a partially coherent light beam passes through the specimen. The light that is diffracted due to phase variations of the specimen and the light that passes without diffraction are then focused together to form a phase contrast image of the specimen. The DIC technique converts changes in the refractive index of the sample into amplitude changes by splitting a polarized beam into two perpendicularly polarized beams less than a micrometer apart. As the index of refraction changes, the phase of the two beams changes after passing through the sample. The two beams are then recombined using a Normaski prism and the recombined beam is sent through an analyzer to form an image of the specimen. The HMC microscopy converts optical phase gradients into amplitude using a spatial filter (or, "modulator"), which has three light-passing zones, a slit plate and a circular polarizer. Different specimen thicknesses deflect the light into different modulator zones thus controlling the contrast of the image. These techniques have well known draw backs such as halo effect (ZPC), shadow effect (DIC), and non-linear phase to amplitude conversion. Because of this non-linearity, phase imaging using these techniques is only qualitative. Quantitative phase imaging is important because it provides information of morphology and refractive indices of specimens. Recently a number of quantitative phase imaging techniques have been developed; Barone-Nugent and team have demonstrated a quantitative phase imaging microscope that separates phase information from amplitude information and produces pure phase images [1], several digital holography techniques have been used for quantitative phase imaging [2, 3], and diffraction phase and fluorescence (DPF) microscopy has been used for simultaneous quantitative phase imaging and epi-fluorescence imaging of living cells [4].

1.1 Phase unwrapping

When the optical depth of an object is greater than the wavelength, the phase image contains 2π ambiguities. Therefore, phase data has to be unwrapped before one can obtain an unambiguous optical thickness profile. Software algorithms that exist for detecting and removing 2π ambiguities are largely computation-intensive and prone to errors when the phase profile is noisy [5]. While the principle of multi-wave phase unwrapping has been known in interferometry [6, 7], known applications have been confined to optical profilers with raster-scanned pointwise interferometry. Other than our recent digital holography experiments [8, 9], multi-wave phase unwrapping has not yet been applied to full-frame phase images. The basic principle of two-wavelength optical phase unwrapping in the context of digital holography was presented by J. Gass, A. Dakoff and M.K. Kim [8]. In this paper, we extend the technique of multi-wavelength optical phase unwrapping to phase-shifting interference microscopy using light emitting diodes at three different wavelengths.

Light emitting diodes (LED) have been used as in interferometric light sources in order to reduce the speckle noise inherent to lasers [10-12]. Interference of coherent waves produces speckle noise, which limits the phase map's information. Since a LED's coherence length is in the micron range, speckle noise is greatly reduced. LEDs also cost much less than lasers, are easy to use and replace and can reduce overall apparatus dimensions. The LEDs used in this experiment are Luxeon™ Emitter diodes from Lumileds Lighting LLC. All of the LEDs used herein have a Lambertian (high dome) radiation pattern. And their spectra are shown in Fig. 1. These spectra were taken with Ocean Optics SD-1000 fiber optics spectrometer.

#83569 - $15.00 USD Received 30 May 2007; revised 10 Jul 2007; accepted 10 Jul 2007; published 12 Jul 2007
(C) 2007 OSA

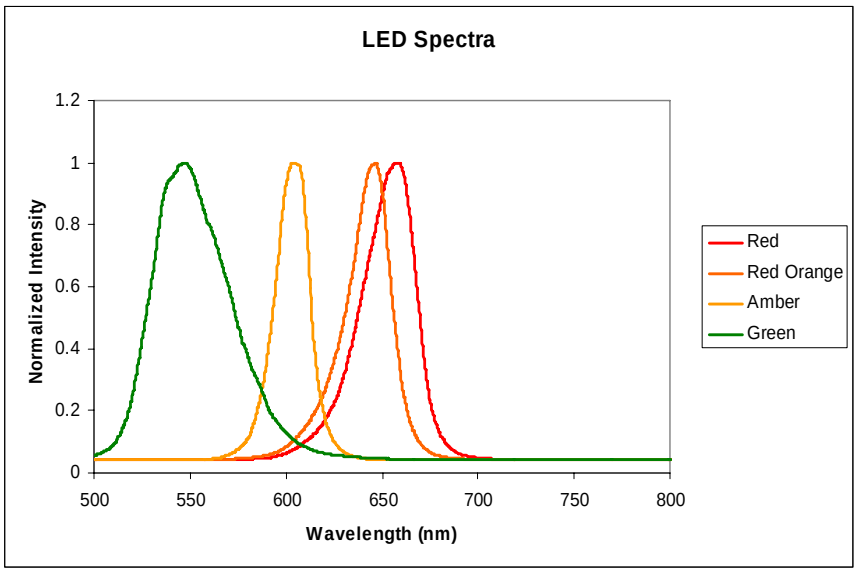

Fig. 1. Spectra for red, red-orange, amber and green LEDs.

The peak wavelengths, luminous flux, calculated and measured coherence lengths for the red, amber and green LEDs used in this experiment are shown in Table 1. The calculated coherence length of a light source is given by $l_C = (2\ln 2/\pi)(\bar{\lambda}^2/\Delta\lambda)$, where $\bar{\lambda}$ is the mean wavelength and $\Delta\lambda$ is the full width half maximum (FWHM) of Gaussian spectrum [13]. The coherence length was directly measured here by counting the number of fringes in the interference of the tilted mirror object.

Table 1. Characteristics of LEDs. Luminous flux values are at 350 mA, Junction Temperature T_J =25^{0}C [14]

Color	Luminous Flux Φ (lm) [14]	Peak Wavelength λ (nm)	Spectral Width (nm)	Calculated Coherence Length (μm)	Measured Coherence Length (μm)
Red	44	653.83 ± 0.07	27.24 ± 0.15	6.91 ± 0.04	9.15 ± 2.45
Red-Orange	55	643.42 ± 0.07	23.21 ± 0.14	7.85 ± 0.05	10.29 ± 2.57
Amber	36	603.48 ± 0.03	17.53 ± 0.05	9.14 ± 0.03	10.86 ± 2.56
Green	25	550.18 ± 0.09	38.93 ± 0.19	3.42 ± 0.02	3.85 ± 1.46

2. Methodology

The experimental setup is shown in Fig. 2. A set of LEDs illuminate a Michelson interferometer. In a fairly standard arrangement, a combination of a polarizing beam-splitter and two quarter-wave plates in the object and reference arms allow all of the reflected light from the two arms to reach the camera. A polarizer-analyzer pair also allows continuous variation of the relative intensity between the two arms. In order to acquire images with high resolution, two 20X microscope objectives are placed in front of the object and the reference mirror. Images acquired by the CCD are sent to an image acquisition board (National Instruments IMAQ PCI^{TM}-1407) installed in the computer.

#83569 - $15.00 USD Received 30 May 2007; revised 10 Jul 2007; accepted 10 Jul 2007; published 12 Jul 2007
(C) 2007 OSA

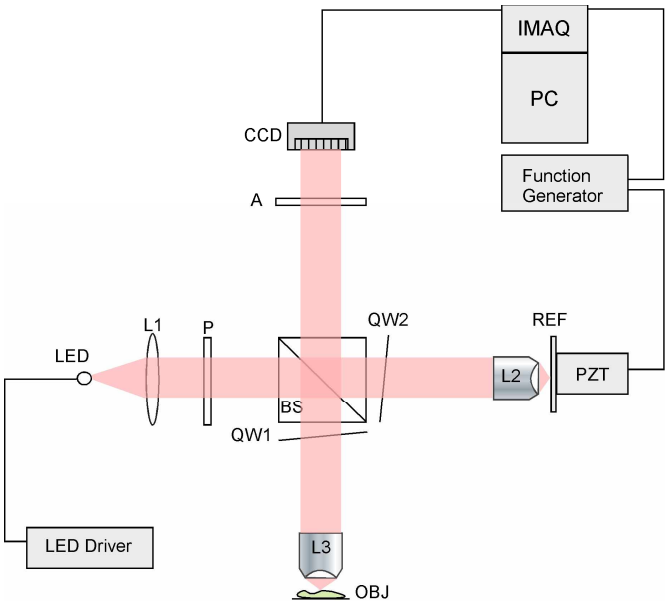

Fig. 2. Experimental setup. L1, collimating lens; L2,L3, microscope objectives; P, polarizer; QW1,QW2, quarter wave plates; A, analyzer; REF, reference mirror, OBJ, object; PZT, piezo transducer; CCD, charged-coupled device camera.

The Intensity *I(x,y)* of the light captured by CCD can be written as;

$$I(x,y) = I_O(x,y) + I_B(x,y) + I_R(x,y) + 2\sqrt{I_O(x,y)I_R(x,y)}\cos[\phi_i + \phi(x,y)] \quad (1)$$

Here $I_O(x, y)$ is the part of the beam reflected by the object that is coherent with respect to $I_R(x,y)$, the intensity of the beam reflected by the reference mirror. $I_B(x, y)$ is part of reflection from the object that is incoherent with respect to the reference – i.e. outside the coherence length. $\phi(x, y)$ is the relative phase between the object and the reference mirror and ϕ_i is the phase shift introduced by moving the reference mirror by quarter wavelength intervals. Four images are acquired at $\phi_i = 0, \pi/2, \pi$ and $3\pi/2$. The phase map of the object is then given by

$$\phi = \tan^{-1}\left[\frac{I_{3\pi/2} - I_{\pi/2}}{I_0 - I_\pi}\right] \quad (2)$$

3. Multi-wavelength optical phase unwrapping

When an object is imaged by using a wavelength smaller than the object's height, the phase image contains 2π ambiguities, as shown in Fig. 3.

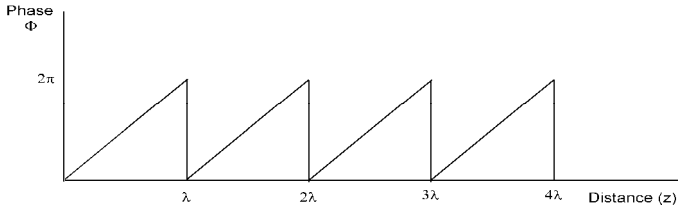

Fig. 3. Phase vs. distance. 2π ambiguities occur when the distance is a multiple of the wavelength.

#83569 - $15.00 USD Received 30 May 2007; revised 10 Jul 2007; accepted 10 Jul 2007; published 12 Jul 2007
(C) 2007 OSA

From Fig. 3, it is clear that there are many distance values for a given phase value. In order to obtain an unambiguous optical thickness profile, we need to have only one z distance for a given phase. These 2π ambiguities are eliminated by using multi-wavelength optical phase unwrapping method. For the mth wavelength λ_m , the surface profile Z_m of an object is related to the phase difference ϕ_m as follows;

$$Z_m = \frac{\lambda_m \phi_m}{2\pi} \tag{3}$$

It is apparent that an unambiguous range of Z can be increased by using a longer λ.

Consider two single wavelength phase maps ϕ_1 and ϕ_2 .The beat wavelength Λ_{12} for λ_1 and λ_2 is given by $\Lambda_{12} = \lambda_1 \lambda_2 / |\lambda_1 - \lambda_2|$. The Λ_{12} can be increased by choosing closer values of λ_1 and λ_2. The phase map for Λ_{12} is obtained by subtracting one single wavelength phase map from the other and then adding 2π whenever the resultant value is less than zero. This phase map is called "coarse map" ϕ_{12}. The surface profile for the coarse map ϕ_{12} is given by $Z_{12} = \Lambda_{12}\phi_{12} / 2\pi$. Note that however, the phase noise in each single wavelength phase map is magnified by the same factor as the magnification of the wavelengths. In the two-wavelength optical phase unwrapping method introduced by J. Gass, *et.al*. [8], the phase noise is reduced by using the following steps.

1. The surface profile Z_{12} is divided into integer multiples of a single wavelength, say λ_1.
2. The result is added to the single wavelength surface profile Z_1.This significantly reduces the phase noise in the coarse map. However, at the boundaries of wavelength intervals λ_1, the noise of the single wavelength phase map appears as spikes.
3. Remove the spikes by comparing the result with the coarse map surface profile Z_{12}.If the difference is more than half of λ_1, addition or subtraction of one λ_1 depending on the sign of the difference removes the spikes.

The resultant 'fine map' has a noise level equal to that of single wavelength surface profile. If a single wavelength phase map ϕ_m contains a phase noise of $2\pi\varepsilon_m$, the two-wavelength phase unwrapping method works properly for $\varepsilon_m < \lambda_m / 4\Lambda_{12}$ [8]. For λ_1 = 653.83 nm and λ_2 = 550.18 nm, the maximum noise limit is $\varepsilon_m \sim 4.7$ %. Using a larger beat wavelength therefore reduces the maximum noise limit.

3.1 Three-wavelength optical phase unwrapping

The advantage of this three wavelength phase unwrapping method is that the beat wavelength can be increased without reducing the maximum noise limit. Suppose the three chosen wavelengths are λ_1 = 653.83 nm, λ_2 = 603.48 nm, and λ_3 = 550.18 nm. The first two wavelengths give a beat wavelength of Λ_{12} = 10.53 μm. Instead of using the surface profile Z_{12} of Λ_{12} = 7.84 μm, which has a high noise, an identical surface profile can be produced by using surface profiles Z_{13} and Z_{23} with beat wavelengths of Λ_{13} = 3.47 μm and Λ_{23} = 6.2 μm, respectively. The resultant "coarse map of coarse maps" ϕ_{13-23} with surface profile $Z_{13\text{-}23}$ also has the same beat wavelength $\Lambda_{13\text{-}23} = \Lambda_{13} \Lambda_{23} / |\Lambda_{13} - \Lambda_{23}| = 7.84$ μm.

The following steps are followed to reduce the noise in $Z_{13\text{-}23}$.

1. The surface profile $Z_{13\text{-}23}$ is divided into integer multiples of one of the wavelengths, say Λ_{13}.
2. The result is added to the surface profile Z_{13}.
3. The resultant map is then compared with $Z_{13\text{-}23}$. If the difference is more than half of Λ_{13}, one Λ_{13} is added or subtracted depending on the sign of the difference.

This approach reduces the phase noise significantly. Any remaining spikes are due to the noise in ϕ_{13}. We call this result the "intermediate fine map" $Z'_{13\text{-}23}$. To reduce the noise in intermediate fine map, we repeat the procedure by dividing $Z'_{13\text{-}23}$ into integer multiples of λ_1 and adding the result to Z_1. Then the resultant map is compared with $Z'_{13\text{-}23}$. If the difference is

#83569 - $15.00 USD Received 30 May 2007; revised 10 Jul 2007; accepted 10 Jul 2007; published 12 Jul 2007
(C) 2007 OSA

more than half of λ_1, one λ_1 is added or subtracted depending on the sign of the difference. Noise in the final map is equal to the noise in single wavelength phase map Z_1. The three wavelength phase unwrapping method works when the maximum noise level ε_m in the single wavelength phase map is the smaller of $\Lambda_{13}/4$ $\Lambda_{12} \sim 11.1\%$ or $\lambda_1/4\Lambda_{13} \sim 4.7\%$. Therefore, the three wavelength phase unwrapping method increases the beat wavelength without magnifying the noise in the final phase map.

4. Experimental results

4.1 Results for two-wavelength optical phase unwrapping

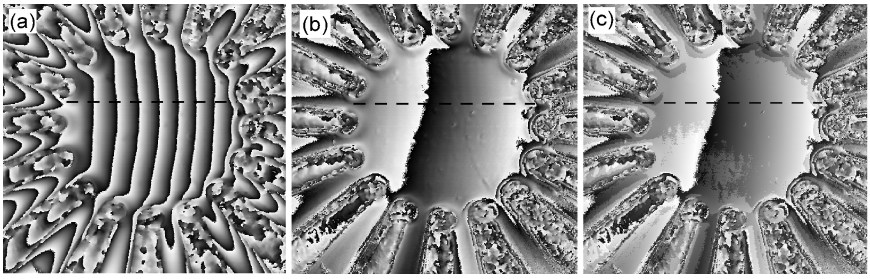

Fig. 4. Results of two-wavelength optical phase unwrapping: (a) single wavelength phase map, (b) two-wavelength coarse map, (c) two-wavelength fine map with reduced noise.

The object here in Fig. 4 is a micro-electrode array biosensor. It consists of 16 gold electrodes on a Pyrex glass substrate. The center is a 125μm diameter circle with an approximate thickness of 2μm. The center of the device was imaged and the experimental results for two-wavelength optical phase unwrapping are shown in Fig. 4. Red (λ_1 = 653.83 nm) and green (λ_2 =550.18 nm) LEDs are used as the two wavelengths. The beat wavelength Λ_{12} = 3.47 μm. Images are of a 184 μm × 184 μm area. Fig. 4(a) shows a single wavelength phase map ϕ_1 with λ_1 = 653.83 nm. The coarse map ϕ_{12} with Λ_{12} = 3.47 μm is shown in Fig. 4(b) and the final phase map with reduced noise is shown in Fig. 4(c). Figure 5 shows cross sections of phase maps along the lines shown in Fig. 4 and the phase noise in the chosen regions. Figure 5(a) is a cross section of single wavelength phase map with λ_1 = 653.83 nm and Fig. 5(b) is a cross section of coarse map with Λ_{12} = 3.47 μm. A cross section of the fine map with reduced noise is shown in Fig. 5(c). For maps (a), (b) and (c), the vertical axis is 4 μm. The root mean square (rms) noise of the coarse map is 43.27 nm. This is shown in Fig. 5(d). Figure 5(e) shows the reduced noise in fine phase map. Since the center of the MEMS device has a curvature, a paraboloid is fitted to the data. The red dotted line is the best-fit parabolic curve. After subtracting the curvature from the data, the Fig. 5(f) shows the corrected phase noise of 10.29 nm.

#83569 - $15.00 USD Received 30 May 2007; revised 10 Jul 2007; accepted 10 Jul 2007; published 12 Jul 2007
(C) 2007 OSA

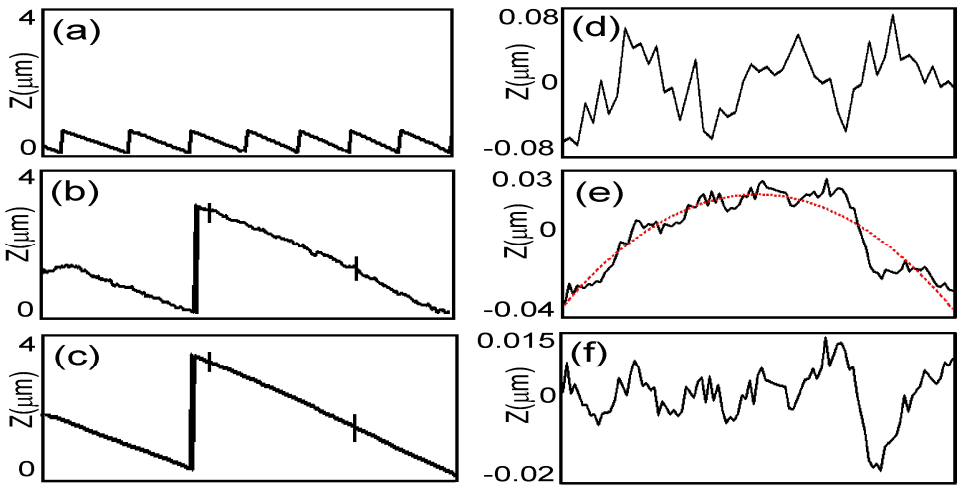

Fig. 5. Surface profiles for two-wavelength phase unwrapping. (a) single wavelength surface profile, (b) surface profile of coarse map, (c) surface profile of final unwrapped phase map with reduced noise, (d) noise of the coarse map in the region between the two markers in plot (b). Rms noise is 43.27 nm, (e) noise of final unwrapped phase map in the area shown in (c). Red dotted line is the best fit parabolic curvature and black solid line is data, (f) corrected phase noise of the unwrapped phase map, after subtracting the curvature of the object. Rms noise is 10.29 nm.

4.2 Results for three-wavelength optical phase unwrapping

The experimental results for three-wavelength optical phase unwrapping are shown in Fig. 6. Red (λ_1= 653.83 nm), amber ((λ_2= 603.48 nm) and green ((λ_3 = 550.18 nm) LEDs are used as the three wavelengths. The beat wavelength Λ = 7.84 μm. The object is the center of the same micro-electrode array bio-sensor used in section (4.1). Images are of a 184 μm × 184 μm area. Figure 6(a) is the single wavelength phase map with λ_1 = 653.83 nm. The three wavelength coarse map is shown in Fig. 6(b) with an equivalent wavelength Λ_{12} = 7.84 μm. The final fine map with reduced noise is shown in Fig. 6(c).

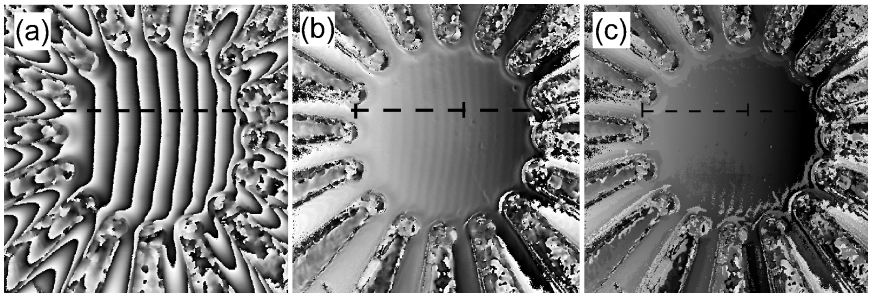

Fig. 6. Results of three-wavelength optical phase unwrapping: (a) single wavelength phase map, (b) three-wavelength coarse map, (c) three- wavelength fine map with reduced noise.

Cross section of each phase map is taken along the lines shown in Fig. 6. These cross sections and phase noise of coarse and fine maps are shown in Fig. 7. Figures 7(a) -7(c) show surface profiles of single wavelength phase map, coarse map and fine map respectively. Vertical axis for each map is 11 μm. Figure 7(d) shows 105.79 nm rms noise of the coarse map. Because of the curvature of the object surface, a paraboloid is fitted with the final fine map data. This is shown in Fig. 7(e). The black line is data and the red dotted line shows the

#83569 - $15.00 USD Received 30 May 2007; revised 10 Jul 2007; accepted 10 Jul 2007; published 12 Jul 2007
(C) 2007 OSA

best- fit parabolic curve. Corrected phase noise in the fine map is 4.78 nm, which is shown in Fig. 7(f).

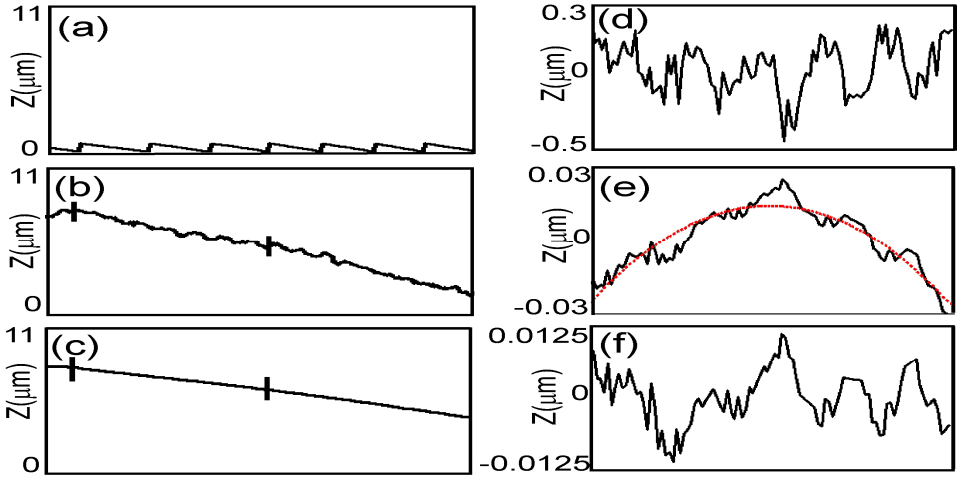

Fig. 7. Surface profiles for three-wavelength phase unwrapping. (a) single wavelength surface profile, (b) surface profile of coarse map, (c) surface profile of final unwrapped phase map with reduced noise. (d) noise of coarse map in the area shown in (b). rms noise is 105.79 nm, (e) noise of final unwrapped phase map in the area shown in (c). Red dotted line is the best fit parabolic curvature and black solid line is data, (f) Final noise of the unwrapped phase map, after subtracting the curvature of the object. Rms noise is 4.78 nm.

The comparison of the two-wavelength phase unwrapping method to the three-wavelength phase unwrapping method shows that the three-wavelength phase unwrapping method increases the axial range of the object, without increasing phase noise. In our results, the two-wavelength phase unwrapping method produced a 3.47 μm unambiguous range with 10.29 nm phase noise, while the three-wavelength phase unwrapping method produced much larger 7.84 μm unambiguous range with smaller 4.78 nm phase noise.

Multi-wavelength optical phase unwrapping method can also be used for biological cells. Figure 8 shows a single wavelength phase map, a coarse map and a fine map of onion cells using red (653.83nm), amber (603.48nm) and green (550.18 nm) wavelengths. The beat wavelength is 7.84 μm. Image size is 184 μm × 184 μm. The Final fine map clearly shows the cell walls by eliminating the 2π ambiguities that would exist in a single wave length phase image.

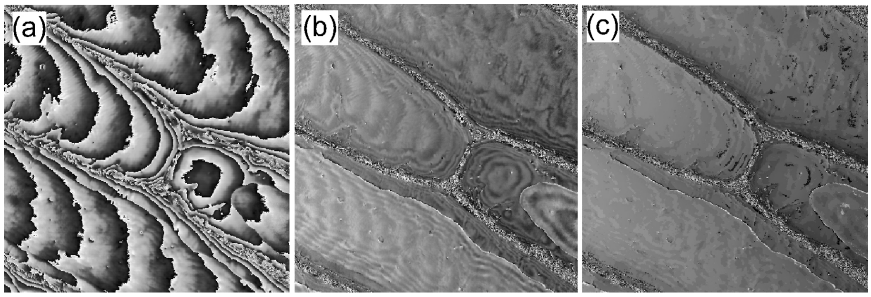

Fig. 8. Results of three-wavelength optical phase unwrapping of onion cells: (a) single wavelength phase map, (b) three-wavelength coarse map, (c) three-wavelength fine map with reduced noise.

#83569 - $15.00 USD Received 30 May 2007; revised 10 Jul 2007; accepted 10 Jul 2007; published 12 Jul 2007
(C) 2007 OSA

5. Conclusions

In conclusion, the effectiveness of multi-wavelength phase imaging for unwrapping phase images with 2π ambiguities has been demonstrated. The three wavelength optical phase unwrapping method can be used to extend the axial range of the object being imaged, without increasing the noise in the phase map. Broadband light sources provide considerably less coherent noise and have added advantages such as lower cost and reduced apparatus dimensions. The multi-wavelength optical phase unwrapping method presented in this paper can be used to check the quality of surface profiles of microscopic objects such as sensors, integrated circuits and many MEMS devices. It can also be used to determine optical thickness profiles of various optical components and biological samples.

Acknowledgment

This work is supported in part by a grant from the National Science Foundation.

#83569 - $15.00 USD Received 30 May 2007; revised 10 Jul 2007; accepted 10 Jul 2007; published 12 Jul 2007
(C) 2007 OSA